

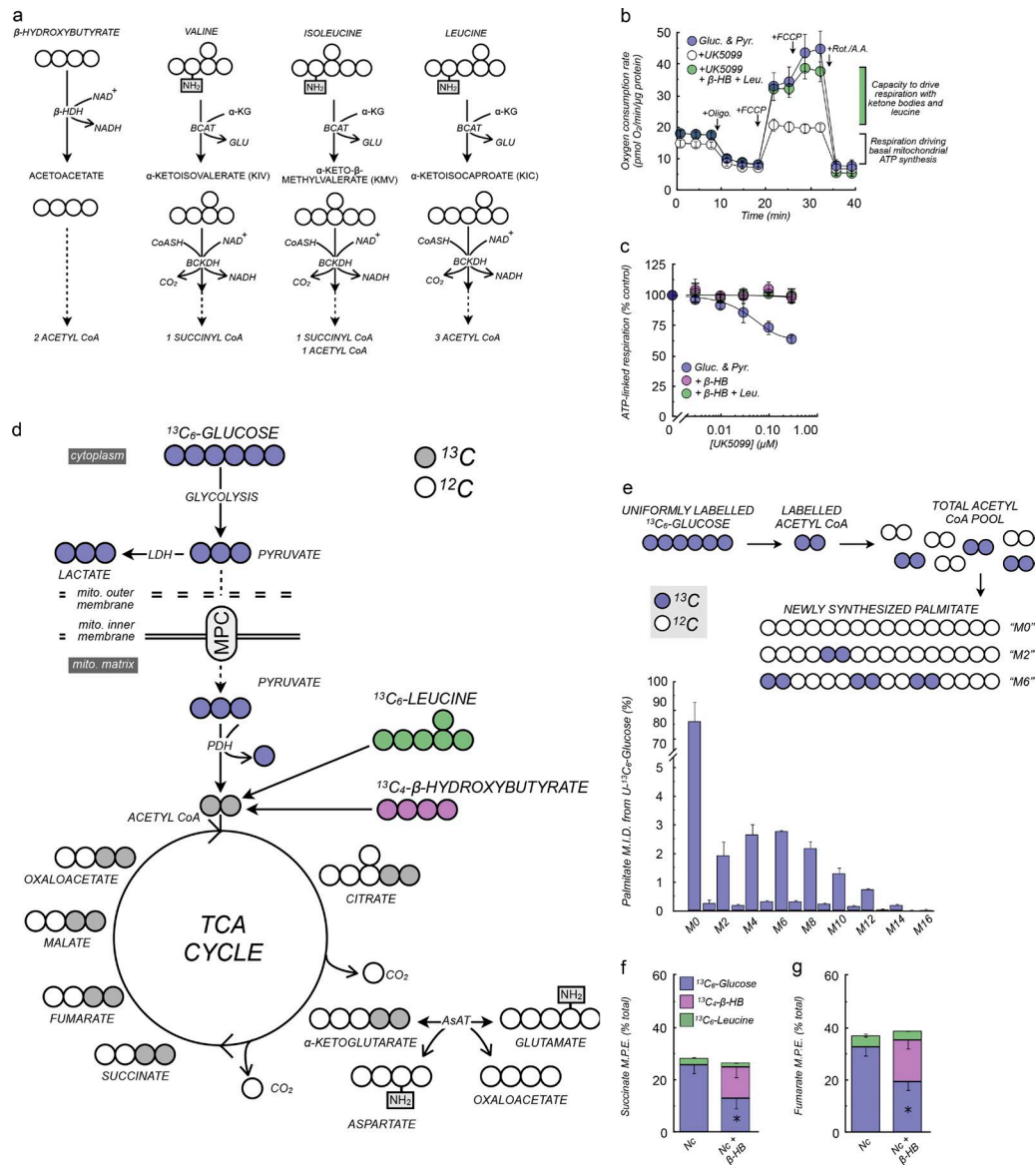
Divakaruni et al., <https://doi.org/10.1083/jcb.201612067>

Figure S1. **Metabolic flexibility in primary cortical neurons.** (a) Oxidation of the ketone body β -hydroxybutyrate generates NADH via β -hydroxybutyrate dehydrogenase (β -HDH) and ultimately produces two acetyl CoA molecules. All branched-chain amino acids are deaminated by the branched-chain aminotransferase (BCAT), and oxidation of the resulting keto acid generates NADH via the branched chain keto acid dehydrogenase (BCKDH). α -KG, α -ketoglutarate. (b) Sample kinetic trace of oxygen consumption shows the capacity of neurons to use nonglucose substrates to fuel respiration. The respiration used to drive basal ATP synthesis is given by oligomycin-sensitive oxygen consumption (white bracket). The maximal respiratory rate driven by β -hydroxybutyrate and leucine can be estimated by the extent to which these substrates can rescue UK5099-inhibited respiration (green bracket); [glucose], 10 mM; [pyruvate], 1 mM; [β -hydroxybutyrate], 3 mM; [leucine], 2 mM; [UK5099], 100 nM. $n = 5$ technical replicates. A.A., antimycin A; Gluc., glucose; Pyr., pyruvate; Rot., rotenone. (c) Concentration–response curve showing that neurons can maintain mitochondrial ATP synthesis upon MPC inhibition by β -hydroxybutyrate (β -HB) and leucine (Leu.) present in the assay medium. Concentrations as in b. $n = 5$. (d) Schematic showing how isotopically labeled glucose (blue), β -hydroxybutyrate (pink), or leucine (green) can be used to measure incorporation from a given substrate into TCA cycle intermediates via generation of acetyl CoA. AsAT, aspartate aminotransferase; LDH, lactate dehydrogenase; mito., mitochondrial; PDH, pyruvate dehydrogenase. (e) Top, isotopomer spectral analysis (ISA) provides a model for understanding how precursor molecules contribute to a newly synthesized, polymerized product. The schematic depicts how acetyl CoA units from a uniformly labeled glucose tracer contribute to de novo palmitate synthesis. Bottom, mass isotopomer distribution (MID) of palmitate from uniformly labeled glucose after 24 h reveals incorporation of two-carbon units into newly synthesized palmitate. $n = 3$ technical replicates \pm SD. (f and g) MPE of labeled carbon into succinate (f) and fumarate (g) shows incorporation of glucose, β -hydroxybutyrate, and leucine into TCA cycle pools. Nc, Neuro-c rich medium; Nc + β -HB, Neuro-c rich medium with 2 mM β -hydroxybutyrate. Data are presented as mean \pm SEM and $n = 4$ unless otherwise stated. *, $P < 0.05$.

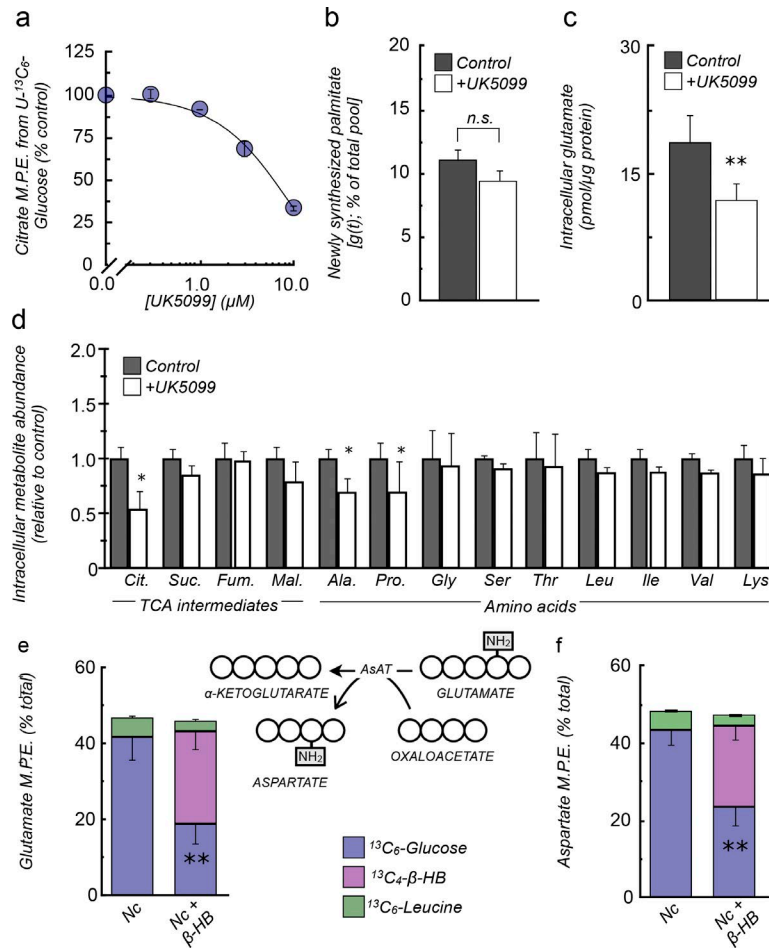


Figure S2. **Inhibition of mitochondrial pyruvate uptake can adjust the abundance and composition of the neuronal glutamate pool while maintaining metabolic rates.** (a) Concentration–response curve of citrate MPE in response to increasing UK5099 concentrations shows that pyruvate carrier inhibition severely restricts glucose incorporation into the TCA cycle. $n = 3$. (b) Newly synthesized palmitate, estimated by isotopomer spectral analysis (ISA), shows that rates of de novo lipogenesis [g(f)] are unchanged by UK5099. Values were calculated using uniformly labeled glucose, β -hydroxybutyrate, and leucine as substrates for each preparation of neurons. (c) Quantitative measurements of glutamate abundance confirm that intracellular levels decrease upon 10 μ M UK5099 treatment for 24 h. (d) For conditions as in c, there is no broad change in levels of amino acids or TCA cycle intermediates apart from decreases in citrate, alanine, and proline. (e and f) MPE of labeled carbon into glutamate (e) and aspartate (f) shows incorporation of glucose, β -hydroxybutyrate, and leucine into TCA cycle pools. Nc, Neuro-c rich medium; Nc + β -HB, Neuro-c rich medium with 2 mM β -hydroxybutyrate; [UK5099], 10 μ M for 24 h. Data are presented as mean \pm SEM and $n = 4$ unless otherwise specified. Ala., alanine; Cit., citrate; Fum., fumarate; Mal., malate; Pro., proline; Suc., succinate. *, $P < 0.05$; **, $P < 0.01$; n.s., not significant.

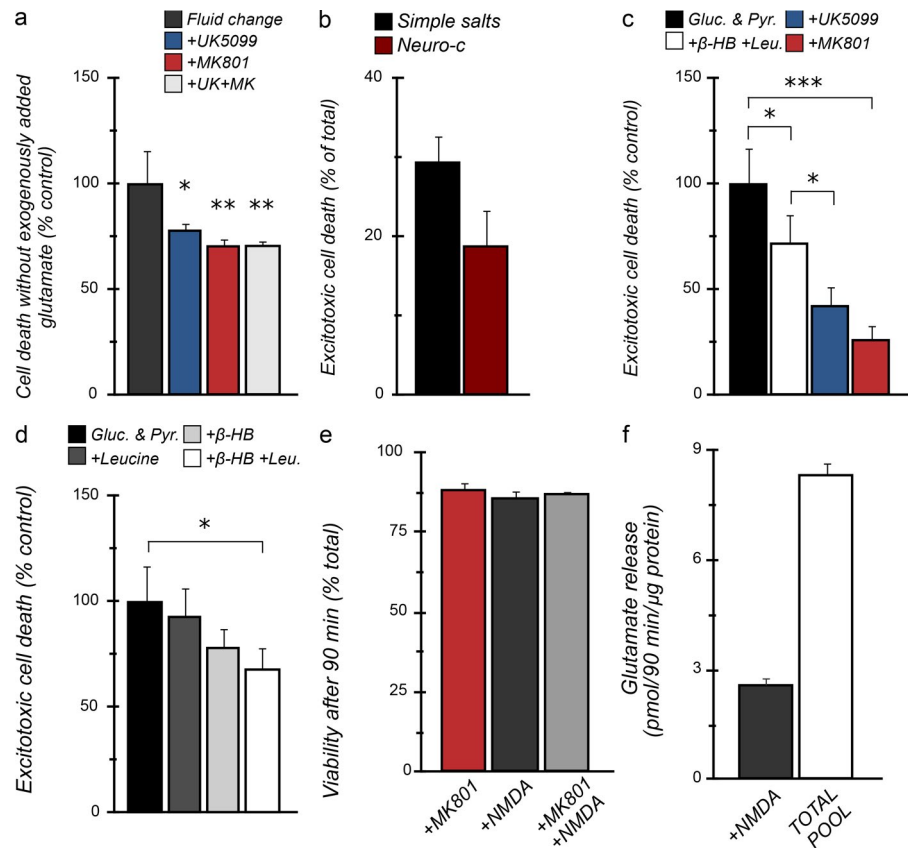


Figure S4. Adjusting neuronal substrate metabolism can protect from glutamate excitotoxicity. (a) Excitotoxic injury in vitro can be mediated by the endogenous glutamate pool. Cell death in the absence of exogenously added glutamate during toxicity assays in Neuro-c rich medium qualitatively reproduces the effects of assays conducted with added glutamate (Fig. 6 c): UK5099 is protective and its effects are not additive to protection afforded by MK801. [UK5099], 10 μ M; [MK801], 10 μ M. (b) Excitotoxicity assays conducted in a simple salts medium cause more excitotoxic cell death, as a percentage of total cells, than assays conducted in Neuro-c rich medium. (c) UK5099 is experimentally neuroprotective in excitotoxicity assays conducted in a simple salts medium: Gluc. & Pyr., 10 mM glucose and 1 mM pyruvate; +β-HB +Leu., 10 mM glucose, 1 mM pyruvate, 2 mM β-hydroxybutyrate, and 2 mM leucine; +UK5099, conditions as in +β-HB +Leu. plus 30 nM UK5099 (medium lacks B27 supplement); +MK801, conditions as in +β-HB +Leu. plus 10 μ M MK801. All treatments received 100 μ M glutamate as detailed in Materials and methods. (d) Supplementing simple salts medium with nonglucose substrates can be protective from excitotoxic injury. Excitotoxic cell death in simple salts medium is presented with labels as in c where applicable. +β-HB, 10 mM glucose, 1 mM pyruvate, and 2 mM β-hydroxybutyrate; +Leu., 10 mM glucose, 1 mM pyruvate, and 2 mM leucine. All treatments received 100 μ M glutamate as detailed in Materials and methods. (e) Neuronal viability is unchanged upon 90-min treatment with 100 μ M NDMA. 10 μ M MK801 was added 30 min before NMDA addition. $n = 3$. (f) Treatment with 100 μ M NDMA for 90 min in Neuro-c evokes release of ~30% of the total releasable glutamate pool. The total releasable pool size was measured by plasma membrane permeabilization with recombinant, mutant PFO ($n = 3$). Data are presented as mean \pm SEM and $n = 4$ unless otherwise noted. *, $P < 0.05$; **, $P < 0.01$; ***, $P < 0.001$.

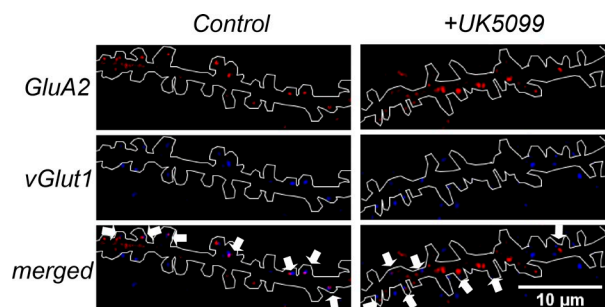


Figure S5. UK5099 treatment does not compromise synaptic density. Representative photomicrograph of immunostaining for GluA2 and vGlut1 in dendritic segments. White curves outline the dendritic segments, and white arrows indicate the colocalized puncta of GluA2 and vGlut1.

Reference

Vacanti, N.M., A.S. Divakaruni, C.R. Green, S.J. Parker, R.R. Henry, T.P. Ciaraldi, A.N. Murphy, and C.M. Metallo. 2014. Regulation of substrate utilization by the mitochondrial pyruvate carrier. *Mol. Cell.* 56:425–435. <http://dx.doi.org/10.1016/j.molcel.2014.09.024>